Inorganica Chimica Acta 394 (2013) 605–615

Contents lists available at SciVerse ScienceDirect

Inorganica Chimica Acta

journal homepage: www.elsevier.com/locate/ica

Metal derivatives of N^1-substituted thiosemicarbazones: Synthesis, structures and spectroscopy of nickel(II) and cobalt(III) complexes

Tarlok S. Lobana [a,*], Poonam Kumari [a], Geeta Hundal [a], Ray J. Butcher [b], A. Castineiras [c], Takashiro Akitsu [d]

[a] Department of Chemistry, Guru Nanak Dev University, Amritsar 143 005, India
[b] Department of Chemistry, Howard University, Washington, DC 20059, USA
[c] Departamento De Quimica Inorganica, Facultad de Farmacia, Universidad de Santiago, 15782 Santiago, Spain
[d] Department of Chemistry, Tokyo University of Science, Tokyo 1628601, Japan

ARTICLE INFO

Article history:
Received 8 February 2012
Received in revised form 17 September 2012
Accepted 20 September 2012
Available online 3 October 2012

Keywords:
Thiosemicarbazone
Nickel(II)
Bis(diphenylphosphino)methane
Cobalt(III)
2-Phenylpyridine

ABSTRACT

Reactions of nickel(II) and cobalt(II) salts with various N^1-substituted thiosemicarbazones [R^{1}R^{2}C^2=N^3–N^{2}H–C^1(=S)–N^{1}HR^3, H$_2$L; R^1 = C$_6$H$_5$-, R^2 = H, H$_2$L^1(R^3 = Me); H$_2$L^2(R^3 = Ph), R^1 = 2-OHC$_6$H$_4$-, R^2 = H, H$_2$L^3(R^3 = Me), H$_2$L^4(R^3 = Et), H$_2$L^5(R^3 = Ph); R^2 = Me, H$_2$L^6(R^3 = Me), R^2 = Me, H$_2$L^7(R^3 = Et) and R^2, R^3 = H, Me, H$_2$L^8(R^1 = C$_4$H$_3$S), H$_2$L^9(R^1 = C$_4$H$_3$O)] are described. Reactions of Ni(OAc)$_2$ with the ligands having R^1 as phenyl group at C^2 carbon (H$_2$L^1, H$_2$L^2) gave complexes, [Ni(κ^2-N^3, S-HL)$_2$] (HL$^-$ = HL^1, **1**; HL^2, **2**). Other ligands with R^1 as 2-hydroxyphenyl groups, namely, H$_2$L^3–H$_2$L^7, with Ni(OAc)$_2$ yielded rust colored compounds, {Ni(κ^3-O, N^3, S–L)} (L^{2-} = L^3–L^7) which after the addition of PPh$_2$-CH$_2$-PPh$_2$ yielded dinuclear, [Ni$_2$(κ^3-O, N^3, S–L)$_2$(μ-P, P–PPh$_2$–CH$_2$–PPh$_2$)] (L^{2-} = L^3, **3**; L^4, **4**; L^5, **5**) and mononuclear, [Ni(κ^3-O, N^3, S–L)(κ^1-P–PPh$_2$–CH$_2$–PPh$_2$)] (L^{2-} = L^6, **6**; L^7, **7**) complexes. Likewise, {Ni(κ^3-O, N^3, S-L^5} with 2-phenylpyridine(2-Phpy) has yielded a mononuclear complex, [Ni(κ^3-O, N^3, S–L^5)(κ^1-N-2-Phpy)] **8**. The geometry around Ni metal center can be formally described as square planar in each of complexes **1**–**8**. Reactions of CoCl$_2$ with H$_2$L^8 and H$_2$L^9 involved oxidation of Co^{II} to Co^{III} and yielded octahedral complexes, [Co(κ^2-N, S–HL)$_3$] (HL$^-$ = HL^8, **9**; HL^9, **10**).

1. Introduction

Thiosemicarbazones {R^{1}R^{2}C^2=N^3–N^{2}H–C^1(=S)–N^{1}HR^3 (I)} represent an interesting class of Schiff bases due to their variable donor ability and structural diversity [1–8]. Applications of thiosemicarbazones as well as their complexes in biology form some of the key motives to pursue their coordination chemistry [1]. Nickel(II) was found to affect the DNA repair mechanisms by inhibiting the base excision repair (BER) and nucleotide excision repair (NER) processes [9,10], which may become a potential merit in the design of antitumor agents. Several nickel(II) complexes have been found to inhibit proliferation of diverse cancer cells [11–13]. For example, a square planar nickel(II) complex of thiophene-2-carbaldehyde thiosemicarbazone was tested against MelanomaB16F10 and FLC cell lines [14] and octahedral nickel(II) complex of phenanthrenequinone thiosemicarbazone was tested on human breast cancer cell line, T47D rich in the progesterone receptors and has a synergistic effect on the antiproliferative activity of the cell lines [15].

The interaction of thiosemicarbazones with several metals such as copper(I), silver(I), gold(I), mercury(II), palladium(II), platinum(II), ruthenium(II) and nickel(II) have yielded mono-, di-, tri- and poly-nuclear complexes [1]. The nature of substituents at C^2 carbon, the type of anion, co-ligands and solvents all influenced bonding and nuclearity of complexes [16]. For example, it was observed that furan-2-carbaldehyde thiosemicarbazones (R^2 = H) with Ni^{II} formed trans-(R^3 = Me, Et) and cis-(R^3 = Ph) square planar complexes, [Ni(κ^2-N, S–HL)$_2$] [17]. For R^2 = methyl, furan ring showed coordination to Ni^{II} and formed octahedral complexes, [Ni(κ^3-O, N, S–HL)$_2$] (R^3 = Me, Et, Ph) [18]. The analogous thiophene thiosemicarbazones (R^2 = H, Me) only formed trans square planar complexes, [Ni(κ^2-N, S–HL)$_2$].

Further, there are limited reports on complexes of nickel(II) with benzaldehyde-/salicylaldehyde-based thiosemicarbazones. The 4-fluorobenzaldehyde thiosemicarbazone formed a square planar complex, [Ni(κ^2-N, S–HL)$_2$] [19], and salicylaldehyde thiosemicarbazones formed either monomers, [Ni(κ^3-O, N^3, S–L)Y] (Y = PPh$_3$, py, NH$_3$) [20–27] or oligomers [Ni(κ^3-O, N^3, S–L)]$_n$ (n = 2, 3) [28,24]. As regards Co$^{II/III}$, in literature, tetrahedral [Co^{II}I$_2$(κ^1-S–H$_2$L)$_2$] (H$_2$L = acetophenone thiosemicarbazone) or octahedral [Co^{III}(κ^3-O, N, S–L)(κ^2-N, N-bipy)(N$_3$)] (L = 2-hydroxy acetophenone thiosemicarbazonate), [Co^{III}(κ^3-O, N, S–HL)$_3$]·4H$_2$O (HL = *N*-(anthracen-9-yl)methyleneamino]thioureate) and [Co^{III}(κ^3-O, N, S–HL)$_3$]·2MeOH (L = *N*-(2-hydroxyethyl)-2-(thiophene-2-ylmethelene)-hydrazinecarbothioamide) complexes are reported [29].

---

[*] Corresponding author. Fax: +91 183 2 258820.
E-mail address: tarlokslobana@yahoo.co.in (T.S. Lobana).

0020-1693/$ - see front matter © 2012 Elsevier B.V. All rights reserved.
http://dx.doi.org/10.1016/j.ica.2012.09.021

Complexes of nickel(II) with the thio-ligands shown in Chart 1 are synthesized using $PPh_2–CH_2–PPh_2$ and 2-Phpy as co-ligands. A few reactions of furan- and thiophene-2-carbaldehyde thiosemicarbazones with cobalt(II) salt are also investigated. Various complexes synthesized have been characterized with the help of analytical data, spectroscopic techniques (IR, ^1H and ^{31}P NMR) and single crystal X-ray crystallography (**1**, **2**, **4** and **7**–**9**).

2. Experimental

2.1. Materials and techniques

Metal salts, namely, $NiCl_2$, $Ni(OAc)_2$, $CoCl_2$, as well as *N*-methyl thiosemicarbazide, *N*-ethyl thiosemicarbazide, *N*-phenyl thiosemicarbazide, benzaldehyde, 2-hydroxybenzaldehyde, 2-hydroxy acetophenone, bis(diphenylphosphino)methane, 2-phenylpyridine and Et_3N were procured from Aldrich Sigma Ltd. The thio-ligands were synthesized by conventional procedures [30]. Elemental analysis for C, H and N were carried out using a thermoelectron FLASHEA1112 analyzer. The melting points were determined with a Gallenkamp electrically heated apparatus. The IR spectra were recorded using KBr pellets on a Varian 666-IR FT-IR spectrometer. ^1H NMR spectra were recorded on a JEOL AL300 FT spectrometer at 300 MHz in $CDCl_3$ with TMS as the internal reference. The ^{31}P NMR spectra were recorded at 121.5 MHz with $P(OMe)_3$ as the external reference.

2.2. Synthesis of complexes

2.2.1. *Trans-[Ni(κ^2-N^3, S–HL^1)$_2$]* (***1***)

To a colorless solution of H_2L^1 (0.038 g, 0.200 mmol) in methanol (10 mL) was added solid $Ni(OAc)_2$ (0.025 g, 0.100 mmol). The color of the solution changed to dark brown and the contents were stirred for about 4 h. The clear solution after filtration was left for slow evaporation at room temperature which gave brown crystals. Yield: 77%; m.p. 192–195 °C. *Anal.* Calc. for $C_{18}H_{20}N_6NiS_2$: C, 48.73; H, 4.51; N, 18.95. Found: C, 48.54; H, 4.33; N, 19.01%. IR (KBr, cm^{-1}, selected absorption bands): $\nu(N^1–H)$ 3387br; ν(C–H), 2987m, 2876m; ν(C=N) + ν(C=C) 1548s, 1497s; ν(C–N) 1067s, 1013s, 875s; ν(C–S) 768s. ^1H NMR (δ, ppm; $CDCl_3$): 8.05 (d, 4H, C^4H & C^8H), 7.45 (s, 2H, C^2H), 7.37 (m, 6H, $C^{5-7}H$), 5.03 (sb, 2H, N^1H), 3.00 (d, 6H, CH_3).

Complex **2** was synthesized by a similar method.

2.2.2. *Trans-[Ni(κ^2-N^3, S–HL^2)$_2$]* (***2***)

Yield: 73%; m.p. 210–212 °C. *Anal.* Calc. for $C_{28}H_{24}N_6NiS_2$: C, 59.22; H, 4.23; N, 14.81. Found: C, 58.99; H, 4.35; N, 14.95%. IR (KBr, cm^{-1}, selected absorption bands): $\nu(N^1–H)$ 3398br; ν(C–H) 3012m, 2998m; ν(C=N) + ν(C=C) 1545s, 1478s; ν(C–N) 1058s, 1017s; ν(C–S) 771s. ^1H NMR (δ, ppm; $CDCl_3$): 8.01 (d, 4H, C^4H & C^8H), 7.61 (s, 2H, C^2H), 7.35 (m, 14H, C^5H & C^7H & *o*- & *p*- & *m*-H), 7.09 (t, 2H, C^6H), 6.89 (sb, 2H, N^1H).

2.2.3. *[Ni$_2$(κ^3-O, N^3, S–L^3)$_2$(μ-P, P–PPh$_2$–CH$_2$–PPh$_2$)]* (***3***)

To a solution of H_2L^3 (0.021 g, 0.100 mmol) in acetonitrile was added solid $NiCl_2$ salt (0.025 g, 0.100 mmol) followed by the addition of Et_3N base (1 mL) and the contents were stirred for 1 h. To this was added solid $PPh_2–CH_2–PPh_2$ (0.039 g, 0.100 mmol) and the contents further stirred for about 4 h and the clear solution was allowed to evaporate at room temperature which yielded red crystals along with the formation of $Et_3NH^+Cl^-$ salt. Yield: 58%; m.p. 210–212 °C. *Anal.* Calc. for $C_{43}H_{40}Ni_2N_6O_2P_2S_2$: C, 56.36; H, 4.40; N, 9.17. Found: C, 56.18; H, 4.61; N, 9.56%. IR (KBr, cm^{-1}, selected absorption bands): $\nu(N^1–H)$ 3412s; ν(C–H) 3049w, 2991w, 2927w, 2878m; ν(C=N) + ν(C=C) 1600s, 1541s; $\nu(P–C_{Ph})$ 1097s; ν(C–N) 1026s, 989s, 916s; ν(C–S) 752s. ^1H NMR (δ, ppm; $CDCl_3$): 8.00 (s, 2H, C^2H), 7.87 (m, 4H, C^5H & C^8H), 7.15 (m, 20H, *o*- & *p*- & *m*-H), 6.54 (m, 4H, C^6H & C^7H), 4.91 (db, 2H, N^1H), 2.86 (s, 2H, CH_2), 2.10 (d, 6H, $CH_3(N^1)$). ^{31}P NMR (δ, ppm; $CDCl_3$): −127.74; coordination shift, $\Delta\delta$ ($\delta_{complex} - \delta_{dppm}$) = 34.93 ($\delta_{dppm}$ = −162.67 dppm).

Complexes **4** and **5** were synthesized by a similar method.

2.2.4. *[Ni$_2$(κ^3-O, N^3, S–L^4)$_2$(μ-P, P–PPh$_2$–CH$_2$–PPh$_2$)]* (***4***)

Yield: 60%; m.p. 215–217 °C. *Anal.* Calc. for $C_{45}H_{44}Ni_2N_6O_2P_2S_2$: C, 57.18; H, 4.66; N, 8.89. Found: C, 56.98; H, 4.45; N, 9.01%. IR (KBr, cm^{-1}, selected absorption bands): $\nu(N^1–H)$ 3419s; ν(C–H) 3078w, 2963w, 2927w, 2867m; ν(C=N) + ν(C=C) 1600s, 1541s; $\nu(P–C_{ph})$ 1097s; ν(C–N) 1045s, 1027s, 999s; ν(C–S) 764s. ^1H NMR (δ, ppm; $CDCl_3$): 7.99 (m, 6H, C^2H, C^5H & C^8H), 7.22 (m, 20H, *o*- & *p*- & *m*-H), 6.50 (m, 4H, C^6H & C^7H), 4.43 (db, 2H, N^1H), 3.27 (m, 4H, $CH_2(N^1)$), 2.01 (s, 2H, CH_2), 1.14 (d, 6H, $CH_3(N^1)$). ^{31}P NMR (δ, ppm; $CDCl_3$): −127.55; coordination shift, $\Delta\delta$ ($\delta_{complex} - \delta_{dppm}$) = 35.11.

2.2.5. *[Ni$_2$(κ^3-O, N^3, S–L^5)$_2$(μ-P, P–PPh$_2$–CH$_2$–PPh$_2$)]·CH$_3$CN* (***5***)

Yield: 59%; m.p. 180–182 °C. *Anal.* Calc. for $C_{55}H_{47}Ni_2N_7O_2P_2S_2$: C, 61.09; H, 4.35; N, 9.07. Found: C, 69.24; H, 4.49; N, 8.87%. IR (KBr, cm^{-1}, selected absorption bands): $\nu(N^1–H)$ 3433br; ν(C–H) 3052m, 2998w; ν(C=N) + ν(C=C) 1602s, 1535s; $\nu(P–C_{Ph})$ 1097s; ν(C–N) 1020s, 996s, 902w; ν(C–S) 745s. ^1H NMR (δ, ppm; $CDCl_3$): 8.20 (s, 2H, C^2H), 7.96 (m, 12H, C^5H & C^8H & N^1Ph-Hs), 7.48–6.94 (m, 20H, *o*- & *p*- & *m*-H), 6.52 (s, 4H, C^6H & C^7H), 6.45 (sb, 2H, N^1H), 3.21 (s, 2H, CH_2). ^{31}P NMR (δ, ppm; $CDCl_3$): −126.61; coordination shift, $\Delta\delta$ ($\delta_{complex} - \delta_{dppm}$) = 36.06.

2.2.6. *[Ni(κ^3-O, N^3, S–L^6)(κ^1-P–PPh$_2$–CH$_2$–PPh$_2$)]* (***6***)

To a light yellow solution of H_2L^6 (0.022 g, 0.100 mmol) in CH_3CN (10 mL) was added solid $Ni(OAc)_2$ (0.025 g, 0.100 mmol) and the contents stirred for 2 h. During stirring rust colored compound got separated and to this was added solid dppm (0.034 g, 0.100 mmol) with a further stirring for 15 min. The color of the solution changed to reddish brown and slow evaporation of the solution formed sticky mass, which was crystallized in methanol. Yield: 69%; m.p. 176–178 °C. *Anal.* Calc. for $C_{35}H_{33}N_3NiOP_2S$: C, 63.28; H, 4.97; N, 6.33. Found: C, 63.45; H, 5.14; N, 6.19%. IR (KBr, cm^{-1}, selected absorption bands): $\nu(N^1–H)$ 3420br; ν(C–H) 3051m, 2925m, 2856w; ν(C=N) + ν(C=C) 1542s, 1483s; $\nu(P–C_{Ph})$

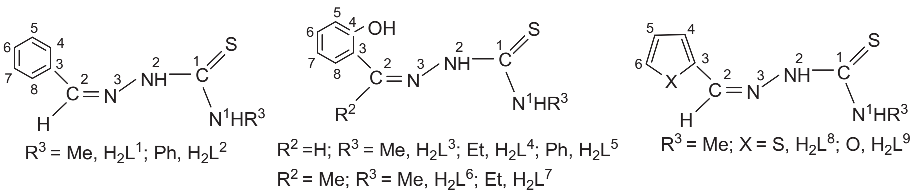

Chart 1.

1099s; ν(C–N) 1068s, 1025m, 915s; ν(C–S) 758s. ^{1}H NMR (δ, ppm; $CDCl_3$): 7.95 (d, 1H, C^5–H), 7.82 (dd, 1H, C^8–H), 7.72–6.97 (m, 20H, *o*- & *p*- & *m*-H), 6.92 (s, 2H, C^6H & C^7H), 4.42 (sb, 1H, N^1H), 3.45 (d, 2H, CH_2), 2.88 (s, 3H, $CH_3(C^2)$), 2.71 (s, 3H, $CH_3(N^1)$). ^{31}P NMR (δ, ppm; $CDCl_3$): −127.73, −166.59; coordination shift, $\Delta\delta$ ($\delta_{complex}$ - − δ_{dppm}) = 34.94, −3.92.

Complexes **7** and **8** were synthesized by a similar method.

2.2.7. [Ni(κ^3-O, N^3, S–L^7)(κ^1-P–PPh_2–CH_2–PPh_2)] (**7**)

Yield: 65%; m.p. 198–200 °C. *Anal.* Calc. for $C_{36}H_{35}N_3NiOP_2S$: C, 63.68; H, 5.16; N, 6.19. Found: C, 63.97; H, 4.98; N, 6.27%. IR (KBr, cm^{-1}, selected absorption bands): ν(N^1–H) 3451br; ν(C–H) 3043m, 2927m, 2878w; ν(C=N) + ν(C=C) 1548s, 1480s; ν(P–C_{Ph}) 1100s; ν(C–N) 1024s; ν(C–S) 763s. ^{1}H NMR (δ, ppm; $CDCl_3$): 7.81 (dd, 1H, C^5H), 7.58 (dd, 1H, C^8H), 7.42–6.78 (m, 20H, *o*- & *p*- & *m*-H), 6.59 (m, 1H, C^6H), 6.45 (dd, 1H, C^7H), 4.48 (sb, 1H, N^1H), 3.30 (m, 2H, $CH_2(N^1)$), 3.17 (d, 2H, CH_2), 2.73 (s, 3H, $CH_3(C^2)$), 1.15 (t, 6H, $CH_3(N^1)$). ^{31}P NMR (δ, ppm; $CDCl_3$): −122.46, −165.14; coordination shift, $\Delta\delta$($\delta_{complex}$ − δ_{dppm}) = 40.21, −2.47.

2.2.8. [Ni(κ^3-O, N^3, S–L^5)(κ^1-N-2-Phpy)] (**8**)

Yield: 72%; m.p. 175–177 °C. *Anal.* Calc. for $C_{25}H_{20}NiN_4OS$: C, 62.08; H, 4.14; N, 11.59. Found: C, 61.92; H, 4.11; N, 12.10%. IR (KBr, cm^{-1}, selected absorption bands): ν(N^1–H) 3436br; ν(C–H) 3105w, 3080w, 2986w; ν(C=N) + ν(C=C) 1598s, 1517s; ν(C–N) 1075s, 1019s, 942w; ν(C–S) 763s. ^{1}H NMR (δ, ppm; $CDCl_3$): 9.56 (s, 1H, C^2H), 8.65 (dd, 2H, C^9H & C^5H), 8.62 (d, 1H, $C^{12}H$), 8.00–7.15 (m, 10H, *o*- *&* *p*- & *m*-H), 7.14 (m, 1H, N^1H), 7.08 (m, 2H, $C^{10}H$ & $C^{11}H$), 6.71 (m, 3H, C^8H & C^6H & C^7H).

2.2.9. [Co(κ^2-N^3, S–L^8)$_3$]·H_2O (**9**)

To a suspension of H_2L^8 (0.063 g, 0.315 mmol) in toluene (10 mL) was added solid $CoCl_2\cdot 6H_2O$ (0.025 g, 0.105 mmol) and the contents stirred for 2 h followed by refluxing for 15 min. During refluxing a black compound got separated along with $Et_3NH^+Cl^-$ salt. Both compounds were separated and crystals for X-ray were grown in CH_2Cl_2 and CH_3OH mixture (3:1::v/v). Yield: 71%; m.p. 150–152 °C. *Anal.* Calc. for $C_{21}H_{26}N_9CoOS_6$: C, 37.51; H, 3.87; N, 18.76. Found: C, 37.89; H, 4.09; N, 18.68%. IR (KBr, cm^{-1}, selected absorption bands): ν(N–H) 3396s; ν(C–H) 3048m, 2957m, 2929br; ν(C=N) + ν(C–C) 1510s, 1403s; ν(C–N) 1045s; ν(C–S) 767s. ^{1}H NMR (δ, ppm; $CDCl_3$): 7.56 (d, 3H, C^2H), 7.40 (m, 3H, C^6H), 7.23 (m, 3H, C^4H), 7.05 (m, 3H, C^5H), 5.22 (sb, 3H, N^1H), 3.25 (d, 9H, CH_3).

Complex **10** was synthesized by a similar method.

2.2.10. [Co(κ^2-N^3, S–L^9)$_3$] (**10**)

Yield: 65%; m.p. 210–212 °C. *Anal.* Calc. for $C_{21}H_{26}N_9CoO_3S_3$: C, 37.51; H, 3.87; N, 18.76. Found: C, 37.89; H, 4.09; N, 18.68%. IR (KBr, cm^{-1}, selected absorption bands): ν(N–H) 3404br; ν(C–H) 3005w, 2959m, 2887w; ν(C=N) + ν(C–C) 1502s, 1402s; ν(C–N) 1084s, 1011s, 945m; ν(C–S) 750s. ^{1}H NMR (δ, ppm; $CDCl_3$): 8.53 (d, 3H, C^2H), 7.63 (q, 3H, C^6H), 7.42 (t, 3H, C^4H), 6.59 (t, 3H, C^5H), 5.25 (sb, 3H, N^1H), 3.09 (d, 9H, CH_3).

2.3. X-ray crystallography

A single crystal was mounted on a glass fiber and used for data collection using a Siemens P4 (**1**), Bruker X8 Kappa APEXII (**2**), Bruker APEX-II CCD (**4**) and Xcalibur, Ruby, Gemini (**7**, **8**) and Bruker SMART CCD 1000 (**9**) diffractometers, equipped with Graphite monochromated Mo Kα (λ = 0.71073 Å). Crystal data were collected at 298(2) (**1**), 100(2) (**2**), 128(2) (**4**), 293(2) (**7**), 123(2) (**8**) and 110(2) (**9**) K. For complex **1**, structure was solved by direct methods and refined by full-matrix least-squares refinement techniques on F^2 using SIR-92 and SHELXL-97 in the Wingx package of programs [31]. Data reduction, structure solution, refinement and

Table 1
Crystallographic data for compounds **1**, **2**, **4** and **7–9.**

	1	**2**	**4**	**7**	**8**	**9**
Empirical formula	$C_{18}H_{20}N_6NiS_2$	$C_{28}H_{24}N_6NiS_2$	$C_{45}H_{44}N_6Ni_2O_2P_2S_2$	$C_{36}H_{35}N_3NiOP_2S$	$C_{25}H_{20}N_4NiOS$	$C_{21}H_{26}CoN_9OS_6$
Formula weight	443.23	567.36	944.34	678.38	483.22	671.80
T (K)	295(2) K	100(2)	128(2)	293(2)	123(2)	100(2)
Crystal system	monoclinic	triclinic	monoclinic	monoclinic	monoclinic	monoclinic
Space group	$C2/c$	$P\bar{1}$	$C2/c$	$P2_1/c$	$P2_1/c$	$P2_1/c$
Unit cell dimensions						
a (Å)	19.749(5)	9.447(5)	19.444(2)	12.007(1)	21.158(4)	10.738(1)
b (Å)	7.474(5)	10.750(6)	8.829(1)	10.239(1)	6.069(1)	29.112(3)
c (Å)	14.628(5)	12.636(6)	24.684(3)	27.191(4)	16.845(3)	9.992(1)
α (°)	90.00	84.357(2)	90.00	90.00	90.00	90.00
β (°)	109.480(5)	75.071(2)	95.10(2)	100.80(2)	90.83(2)	114.96(2)
γ (°)	90.00	84.480(2)	90.00	90.00	90.00	90.00
V (Å^3)	2035.6(2)	1230.63(1)	4220.6(8)	3283.4(8)	2162.5(7)	2831.7(5)
Z	4	2	4	4	4	4
D_{calc} (g cm^{-3})	1.446	1.531	1.486	1.372	1.484	1.576
μ (mm^{-1})	1.173	0.990	1.114	0.786	1.020	1.083
F(000)	920	588	1960	1416	1000	1384
Crystal size (mm^3)	0.20 × 0.10 × 0.10	0.67 × 0.08 × 0.08	0.40 × 0.30 × 0.25	0.46 × 0.35 × 0.24	0.49 × 0.23 × 0.18	0.37 × 0.30 × 0.29
Reflections collected	1946	25885	12649	30228	27298	33631
Unique reflections (R_{int})	1889 (0.0226)	5042 (0.0518)	4848 (0.0271)	11040 (0.0789)	13819 (0.0249)	6068 (0.0512)
Data/restraints/parameters	1889/0/128	5042/0/334	4848/0/272	11040/0/399	13819/0/289	6068/0/343
Index ranges	$0 \leqslant h \leqslant 23$, $0 \leqslant k \leqslant 9$, - $17 \leqslant l \leqslant 16$	$-11 \leqslant h \leqslant 11$, $-13 \leqslant k \leqslant 13$, $0 \leqslant l \leqslant 15$	$-22 \leqslant h \leqslant 25$, $-11 \leqslant k \leqslant 9$, $-31 \leqslant l \leqslant 32$	$-13 \leqslant h \leqslant 17$, $-15 \leqslant k \leqslant 15$, $-36 \leqslant l \leqslant 41$	$-38 \leqslant h \leqslant 32$, $-11 \leqslant k \leqslant 11$, $-30 \leqslant l \leqslant 30$	$-13 \leqslant h \leqslant 12$, $0 \leqslant k \leqslant 36$, $0 \leqslant l \leqslant 12$
Final R indices[$I > 2\sigma(I)$]	R_1 = 0.0463, wR_2 = 0.1201	R_1 = 0.0343, wR_2 = 0.0696	R_1 = 0.0340, wR_2 = 0.1038	R_1 = 0.0645, wR_2 = 0.1445	R_1 = 0.0424, wR_2 = 0.0901	R_1 = 0.0365, wR_2 = 0.0793
R indices (all data)	R_1 = 0.0657, wR_2 = 0.1267	R_1 = 0.0505, wR_2 = 0.0779	R_1 = 0.0428, wR_2 = 0.1133	R_1 = 0.1231, wR_2 = 0.1577	R_1 = 0.0624, wR_2 = 0.0988	R_1 = 0.0525, wR_2 = 0.0856
Largest difference peak and hole (e Å^{-3})	0.732 and −0.640	0.362 and −0.372	0.499 and −0.249	1.457 and −0.491	0.634 and −0.493	0.807 and −0.397

Table 2
Bond parameters of compounds **1**, **2**, **4** and **7–9.**

Compound ***1***			
Ni–N(1)	1.906(3)	Ni–S(1)	2.1819(1)
C(7)–N(1)	1.296(5)	C(8)–S(1)	1.744(4)
N(1)–Ni–S(1)	85.26(9)	N(1)$^{\#1}$–Ni–S(1)	94.74(9)
N(1)$^{\#1}$–Ni–N(1)	180	S(1)–Ni–S(1)$^{\#1}$	180
Compound ***2***			
Ni(1)–N(12)	1.924(2)	Ni(1)–N(22)	1.9223(2)
Ni(1)–S(1)	2.175(6)	Ni(1)–S(2)	2.179(6)
N(12)–C(17)	1.297(3)	N(22)–C(27)	1.301(3)
S(1)–C(18)	1.739(2)	S(2)–C(28)	1.736(2)
N(12)–Ni(1)–S(1)	85.55(5)	N(22)–Ni(1)–S(2)	85.47(5)
N(12)–Ni(1)–S(2)	95.27(5)	N(22)–Ni(1)–S(1)	93.80(5)
S(1)–Ni(1)–S(2)	175.89(3)	N(22)–Ni(1)–N(12)	178.62(8)
Compound ***4***			
Ni(1)–O(1)	1.845(1)	Ni(1)–N(1)	1.889(2)
Ni(1)–S(2)	2.122(6)	Ni(1)–P(1)	2.197(5)
S(2)–C(8)	1.756(2)	N(1)–C(7)	1.297(2)
O(1)–Ni(1)–N(1)	95.62(6)	N(1)–Ni(1)–S(2)	87.40(5)
O(1)–Ni(1)–P(1)	82.62(4)	S(2)–Ni(1)–P(1)	94.20(2)
O(1)–Ni(1)–S(2)	176.51(5)	N(1)–Ni(1)–P(1)	174.49(5)
Compound ***7***			
Ni–O(1)	1.838(2)	Ni–N(1)	1.902(2)
Ni–S	2.143(9)	Ni–P(1)	2.196(8)
S–C(9)	1.745(3)	N(1)–C(7)	1.304(3)
O(1)–Ni–N(1)	95.07(9)	N(1)–Ni–S	88.19(7)
O(1)–Ni–P(1)	85.55(6)	S–Ni–P(1)	90.97(3)
O(1)–Ni–S	174.73(7)	N(1)–Ni–P(1)	176.82(7)
Compound ***8***			
Ni–O(1A)	1.854(8)	Ni–N(1A)	1.861(9)
Ni–N(1B)	1.930(9)	Ni–S	2.147(3)
S–C(8A)	1.742(1)		
O(1A)–Ni–N(1A)	96.06(4)	O(1A)–Ni–N(1B)	86.18(4)
N(1A)–Ni–S	87.34(3)	N(1B)–Ni–S	91.65(3)
N(1A)–Ni–N(1B)	172.15(4)	O(1A)–Ni–S	170.40(3)
Compound ***9***			
Co(1)–N(22)	1.949(2)	Co(1)–N(12)	1.954(2)
Co(1)–N(32)	1.973(2)	Co(1)–S(12)	2.221(7)
Co(1)–S(32)	2.223(7)	Co(1)–S(22)	2.231(7)
S(11)–C(11)	1.711(3)	S(11)–C(14)	1.722(3)
S(12)–C(16)	1.743(3)	N(22)–C(25)	1.299(3)
N(32)–C(35)	1.305(3)	N(12)–C(15)	1.289(3)
N(22)–Co(1)–N(12)	93.73(8)	N(22)–Co(1)–N(32)	93.24(8)
N(12)–Co(1)–N(32)	93.19(8)	N(22)–Co(1)–S(12)	91.35(6)
N(12)–Co(1)–S(12)	86.11(6)	N(12)–Co(1)–S(32)	89.71(6)
N(32)–Co(1)–S(32)	85.82(6)	S(12)–Co(1)–S(32)	89.62(3)
N(22)–Co(1)–S(22)	84.94(6)	N(32)–Co(1)–S(22)	89.76(6)
S(12)–Co(1)–S(22)	91.04(3)	S(32)–Co(1)–S(22)	91.65(3)
N(32)–Co(1)–S(12)	175.39(6)	N(22)–Co(1)–S(32)	176.47(6)
N(12)–Co(1)–S(22)	176.83(7)		

Table 3
Hydrogen bonds (Å) for Complexes **1**, **2**, **4** and 7–9.

Complex No.	D–H···A	d(D–H)	d(H···A)	d(D···A)	⟨(DHA)
1	C(9)–H(9A)···Ni	0.960	2.620	3.540(5)	160.62
	N(3)–H(31)···N(2)$^{\#1}$	0.825	2.450	3.201(5)	151.75
	C(9)–H(9C)···S(1)$^{\#1}$	0.960	2.920	3.843(5)	161.50
2	N(24)–H(24A)···S(1)	0.890	3.010	3.676(2)	133.20
	C(15)–H(15)···C(22)	0.950	2.865	3.766	158.70
	C(15)–H(15)···C(21)	0.950	2.763	3.578	144.26
	C(10)–H(10)···C(26)	0.950	2.826	3.300	111.85
4	C(19) –H(19)···S(2)	0.950	2.881	3.533	126.86
	N(3)–H(3D)···C(19)	0.711	2.734	3.432	167.43
	C(10)–H(10B)···C(22)	0.980	2.865	3.797	159.41
7	C(15)–H(15A)···N(2)	0.929	2.450	3.375	173.04
8	C(10B)–H(8BA)···S	0.950	2.971	3.837	152.34
	C(1B)–H(1BA)···C(1A)	0.950	2.769	3.320	117.80
	C(1B)–H(1BA)···C(2A)	0.950	2.784	3.474	130.14
	C(1B)–H(1BA)···C(3A)	0.950	2.851	3.730	154.38
	C(1B)–H(1BA)···C(4A)	0.950	2.883	3.831	175.42
	C(1B)–H(1BA)···C(5A)	0.950	2.873	3.710	147.63
	C(1B)–H(1BA)···C(6A)	0.950	2.847	3.488	125.67
	N(3A)–H(3AB)···C(12A)	0.880	2.864	3.470	127.48
	N(3A)–H(3AB)···C(13A)	0.880	2.725	3.547	156.01
	C(14A)–H(14A)···C(9A)	0.949	2.766	3.625	150.91
9	N(14)–H(14A)···S(32)	0.750	2.830	3.566(2)	167.80
	N(34)–H(34A)···O(1)	0.880	2.060	2.891(3)	158.20
	O(1)–H(1B)···S(32)	0.960	2.850	3.811(3)	177.50

molecular graphics were performed using SHELXTL-PC [32] and WINGX [33]. The data were processed with APEX2 and corrected for absorption using SADABS [34] for complexes **2**, **4** and CRYSALISPRO CCD (data collection), CRYSALISPRO RED (cell refinement, data reduction) [35] for complexes **7** and **8**. For complex **9**, data were processed with SAINT [36] and corrected for absorption using SADABS [34]. The structures were solved by direct methods using the program SHELXS-97 and refined by full-matrix least-squares techniques against F^2 using SHELXL-97 [31]. Atomic scattering factors were taken from "International Tables for Crystallography" [37]. Molecular graphics were taken from PLATON [38] and SCHAKAL [39]. The crystallographic data and important bond parameters and H-bonds of complexes (**1**, **2**, **4**, **7**, **8** and **9**) are given in Tables 1–3 respectively.

3. Results and discussion

3.1. Syntheses and IR spectroscopy

Schemes 1–3 depict the formation of complexes **1**–**10**. The reactions of $Ni(OAc)_2$ with H_2L^1 and H_2L^2 in 1:2 M ratio (M:L) in methanol formed a clear brown solution in each case which on slow evaporation yielded complexes of stoichiometry, $[Ni(\kappa^2\text{-N, S–HL})_2]$ ($HL^- = HL^1$, **1**; HL^2, **2**). Here, the deprotonation of $–N^2H–$ group occurred and the ligands coordinate as uninegative bidentate anions. The same products were obtained when reactions were performed in 1:1 M ratios. The $PPh_2–CH_2–PPh_2$ did not show coordination to Ni^{II} in complexes **1** and **2**. Reactions of $NiCl_2$ with the thio-ligands, H_2L^3, H_2L^4 and H_2L^5 in the presence of Et_3N base using $PPh_2–CH_2–PPh_2$ as co-ligand gave clear solutions in each case and from which crystals of dinuclear complexes, $[Ni_2(\kappa^3\text{-O, N}^3\text{, S–L})_2(\mu\text{-P, P–PPh}_2\text{–CH}_2\text{–PPh}_2)]$ ($L = L^3$, **3**; L^4, **4**; and L^5, **5**) were obtained. For $R^2 = Me$, the addition of $PPh_2–CH_2–PPh_2$ to the brown suspension of $\{Ni(\kappa^3\text{-O, N}^3\text{, S–L})\}$ ($L^{2-} = L^6$, L^7) in CH_3CN (obtained from $Ni(OAc)_2$ and the thio-ligands, H_2L^6, H_2L^7) formed reddish brown solution from which complexes of stoichiometry, $[Ni(\kappa^3\text{-O, N}^3\text{, S–L})(\kappa^1\text{-P–PPh}_2\text{–CH}_2\text{–PPh}_2)]$ ($L^{2-} = L^6$, **6**; L^7, **7**) were obtained. Further, reactions of 2-Phpy with $\{Ni(\kappa^3\text{-O, N}^3\text{, S–L}^5)\}$ in acetonitrile gave crystals of composition, $[Ni(\kappa^3\text{-O, N}^3\text{, S–L}^5)(\kappa^1\text{-N-2-Phpy})]$ **8**. This coordination behavior is similar to that of pyridine [20]. Reactions of $CoCl_2$ with heterocyclic thiosemicarbazones (H_2L^8, H_2L^9) in the presence of triethyl amine base was anticipated to form tetrahedral complexes of composition, $[Co(\kappa^2\text{-N, S–HL})_2]$. However, during crystallization, Co^{II} got oxidized to Co^{III} and yielded octahedral complexes of stoichiometry, $[Co(\kappa^2\text{-N, S–HL})_3]$ ($HL^- = HL^8$, **9**; HL^9, **10**).

IR spectroscopy revealed deprotonation of $–N^2H–$ group in complexes **1**–**10**. In addition, the –OH group is also deprotonated during formation of complexes **3**–**8** which is further confirmed by the single crystal X-ray crystallography (vide infra). The diagnostic ν(C–S) bands (745–771 cm^{-1}) show low energy shift vis-à-vis the free ligands (809–821 cm^{-1}) and suggested that thio-ligands

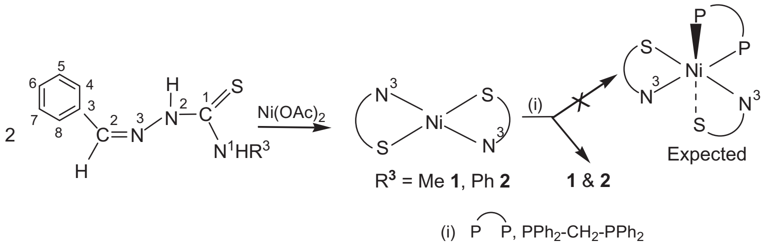

Scheme 1.

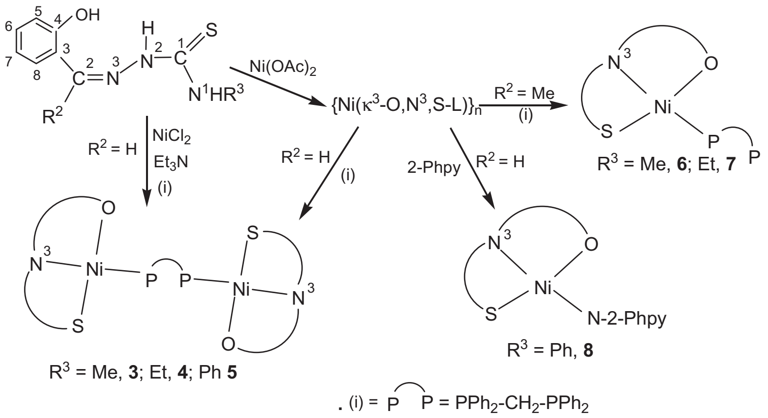

Scheme 2.

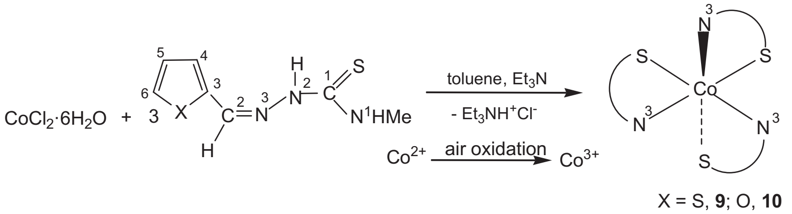

Scheme 3.

coordinate to the metal centers through thiolato sulfur atoms [17,20]. The presence of tertiary phosphine is supported by its characteristic $\nu(\text{P–C}_{\text{Ph}})$ bands in the range, 1097–1100 cm^{-1} (see Section 2).

3.2. Crystal structures

The crystal structure of $[\text{Ni}(\kappa^2\text{-N, S–HL}^1)_2]$ **1** complex has shown that two uninegative $(\text{HL}^1)^-$ ligands chelate to nickel(II) metal center through azomethine nitrogen (N) and thiolato sulfur (S) atoms in trans-N_2S_2 fashion forming the five membered rings (Fig. 1). The bond distances, Ni–N1 {1.906(3) Å} and Ni–S1 {2.182(1) Å}, are similar to those in a related complex, $[\text{Ni}(\kappa^2\text{-N, S–HL}^9)_2]$ {Ni–N, 1.926(2); Ni–S, 2.175(9) Å} [17,40]. The parameters, C8–S1 bond length, the N1···C8 distance and the N1–N2–C8 angle, have been used for distinguishing between anionic and neutral coordinated thiosemicarbazone ligands. These parameters {angle N1–N2–C8, 110.64°; distance N1···C8, 2.231 Å and bond length C8–S1, 1.74 Å} are similar to those for complexes with anionic thiosemicarbazone ligands reported in literature [40a]. Further C8–S1 bond distance {1.744(4) Å} shows a partial double bond character {C–S, 1.81; C=S 1.62 Å) as observed earlier for such thiosemicarbazone complexes [1,40]. Trans angles, N–Ni–N and S–Ni–S {1 8 0}, suggest a square planar geometry with nickel(II) located on inversion center with perfectly coplanar NiSCN_2 planes.On changing R^3 = Ph in place of Me at N^1 nitrogen in H_2L^2, again trans square planar complex, $[\text{Ni}(\kappa^2\text{-N, S–HL}^2)_2]$ **2** has been obtained, which is similar to **1** (Fig. 2). In complex **2**, the trans bond angles N–Ni–N and S–Ni–S are 178.62(8)° and 175.89(3)° respectively suggesting a slight deviation from the regular square planar geometry. Other bond parameters are similar to those found in **1**.

For R^2 = H at C^2 carbon and R^3 = Et at N^1 atom, H_2L^4, the dinuclear complex, $[\text{Ni}_2(\kappa^3\text{-O, N, S–L}^4)_2(\mu\text{-P, P–PPh}_2\text{–CH}_2\text{–PPh}_2)]$ **4** has been obtained. Here, each nickel(II) ion is coordinated to a dinegative $(\text{L}^4)^{2-}$ thio-ligand through O, N and S atoms and two such three coordinated units are bridged by $\text{PPh}_2\text{–CH}_2\text{–PPh}_2$ ligand (Fig. 3). The bond distances around two nickel centers are similar {Ni(1)–O(1), 1.845(1); Ni(1)–N(1), 1.889(2); Ni(1)–S(2), 2.122(6); Ni(1)–P(1), 2.197(5) Å}. These parameters are similar to those of complex, $[\text{Ni}(\kappa^3\text{-O, N, S–L}^3)(\text{PPh}_3)]$, reported in the literature [19]. The O, N and S donor atoms have formed six and five membered chelate rings with the bite angles, O(1)–Ni(1)–N(1) and N(1)–Ni(1)–S(2) of 95.62(6)° and 87.40(5)° respectively and are similar to those reported in the literature [19]. The trans bond angles O(1)–Ni(1)–S(2) and N(1)–Ni(1)–P(1) are 176.51(5)° and 174.49(5)° respectively and suggest a distortion from a regular

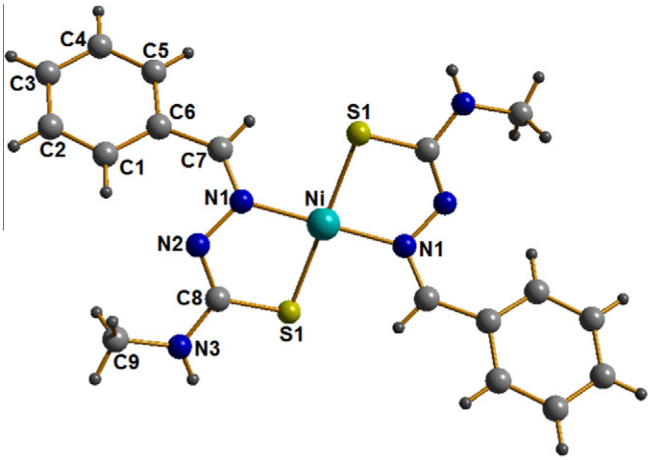

Fig. 1. Molecular structure of complex [Ni(κ^2-N, S–HL^1)$_2$] **1** (Note: The carbon and nitrogen atoms are numbered differently in Chart 1 and Schemes 1–3 from those in molecular structures of **1**, **2**, **4**, and **7**–**9**).

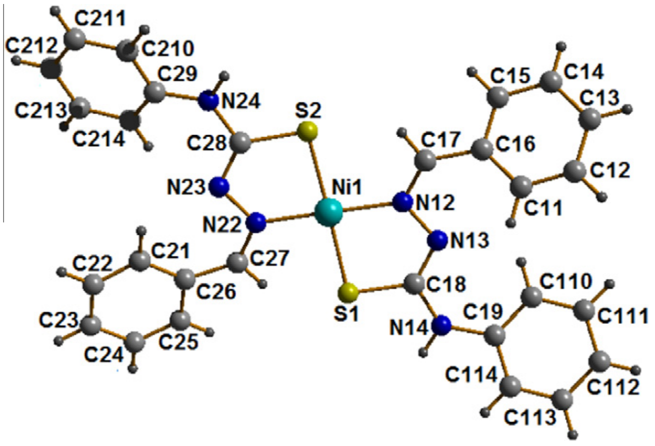

Fig. 2. Molecular structure of complex [Ni(κ^2-N, S–HL^2)$_2$] **2**.

square planar geometry. Further, Ni···Ni separation (5.573 Å) is much longer than twice the sum of the van der Waals radius of nickel atoms, 3.26 Å [41]. The introduction of methyl group (R^2 = Me in place of H) at C^2 carbon with R^3 = Et, the thio-ligand H_2L^7 formed a mononuclear complex, [Ni(κ^3-O, N, S–L^7)(κ^1-P–PPh_2–CH_2–PPh_2)] **7**. In this complex, the dinegative thio-ligand $(L^7)^{2-}$ coordinated to the metal center through O, N and S donor atoms. The fourth coordination site is occupied by P atom of PPh_2–CH_2–PPh_2 co-ligand (Fig. 4). Unlike that in complex **4**, here one PPh_2 group is pendant. The bond distances, Ni–O(1) {1.838(2) Å}, Ni–N(1) {1.902(2) Å}, Ni–S {2.143(9) Å}, Ni–P(1) {2.196(8) Å} are close to those found in complex **4**. Trans angles {174.73(7), 176.82(7)°} suggest a distorted square planar geometry around the metal center.

The 2-pyridylphenyl co-ligand is coordinated to Ni(II) in complex, [Ni(κ^3-O, N, S–L^5)(κ^1-N-2-Phpy)] **8**. Here, the dinegative thiosemicarbazone ligand $(L^5)^{2-}$ is bonded to the nickel(II) center through O, N, S donor atoms and formed six and five membered chelate rings (Fig. 5). It was expected that nickel(II) might metallate to 2-pyridylphenyl and form C, N-chelate bond or simply show coordination similar to pyridine. It however showed simple coordination by pyridyl nitrogen and formed a square planar complex (**8**) similar to pyridine complex [Ni(κ^3-O, N, S–L^3)(κ^1-N-py] [20]. However, the bond parameters in **8** are slightly different than those found in pyridine complex in literature [20]. For example, the bond distance, Ni–O {1.853(8) Å}, is smaller and Ni–$N_{2\text{-Phpy}}$ {1.930(9) Å} is longer {1.907(1) and 1.745(2) Å} [20]. The trans angles, 172.15(4)° and 170.40(3)°, suggest distorted square planar geometry.

Finally, X- ray crystal structure of complex, [Co(κ^2-N, S–HL^8)$_3$]·H_2O (**9**), shows that three uninegative $(HL^8)^-$ ligands are coordinated to cobalt(III) center via sulfur and azomethine nitrogen atoms (Fig. 6). The bond lengths Co–$N_{(\text{azomethine})}$ {1.954(2), 1.949(2), 1.973(2) Å} and Co–S {2.221(7), 2.231(7), 2.223(7) Å} are close to those observed in bis complex, [CoL_2](NO_3)·H_2O (L = pyridine-2-carbaldehyde-*N*-phenylethylthiosemicarbazonate) {Co–N, 1.885(5), 1.876(5); Co–S, 2.232(2), 2.204(2) Å} [42]. The C–S bond distances, (1.711(3), 1.722(3), 1.743(3) Å) are close to those found in the literature [42]. The trans angles, N(32)–Co(1)–S(12), 175.39(6)°; N(32)–Co(1)–S(32), 176.47(6)° and N(12)–Co(1)–S(22), 176.83(7)°, reveal a slight distortion from an octahedral geometry.

3.3. H-bonded networks

In complex **1**, the phenyl group present at C(7) carbon is not engaged in the intermolecular interactions and the polymeric

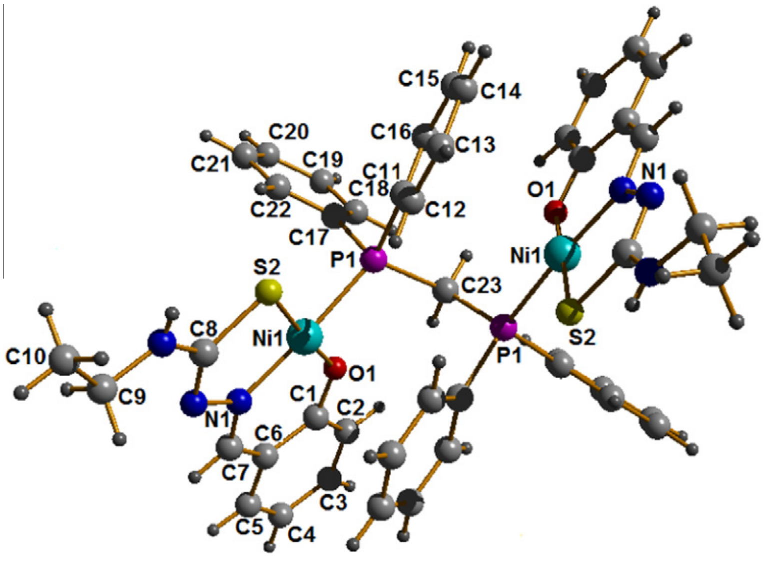

Fig. 3. Molecular structure of complex [Ni_2(κ^3-O, N, S–L^4)$_2$(μ-P, P–PPh_2–CH_2–PPh_2)] **4**.

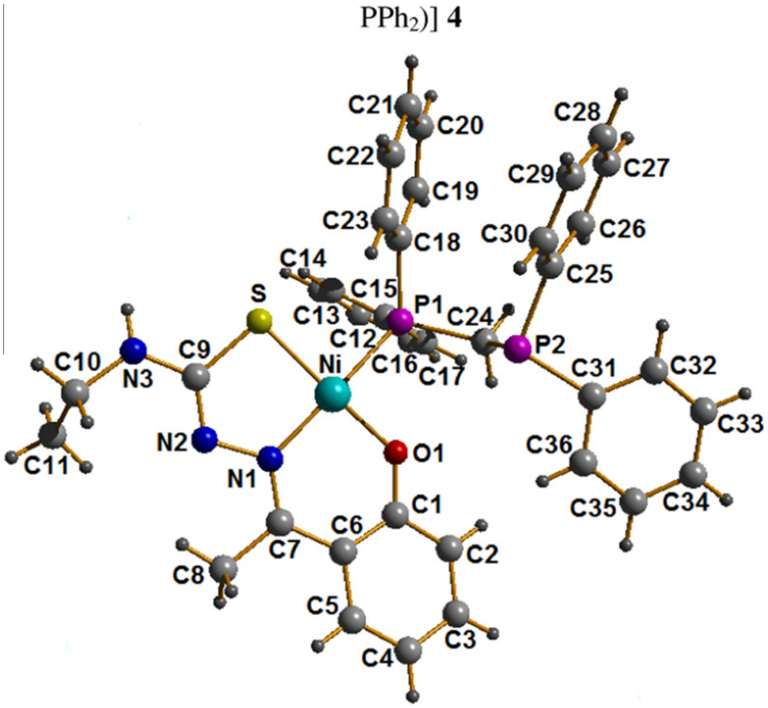

Fig. 4. Molecular structure of complex [Ni(κ^3-O, N, S–L^7)$_2$(κ^1-P–PPh$_2$–CH$_2$–PPh$_2$)] **7**.

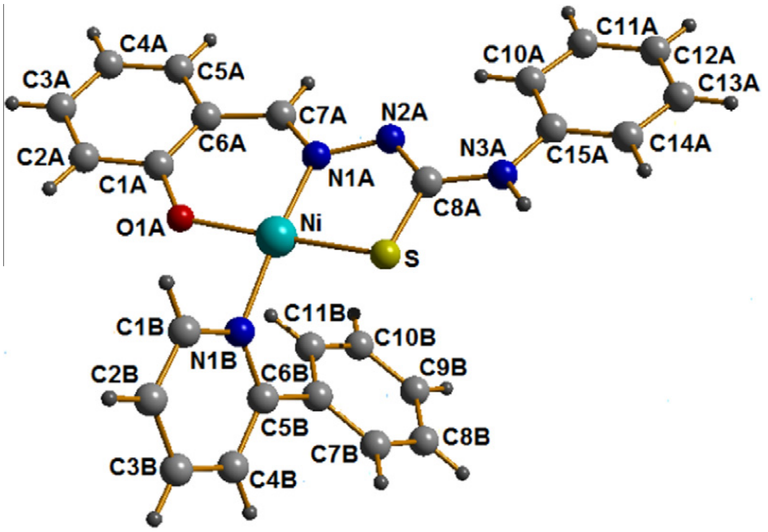

Fig. 5. Molecular structure of complex [Ni(κ^3-O, N, S–L^5)$_2$(κ^1-N–Phpy)] **8**.

network is formed via N(3)–H(31)···N(2)$^{\#1}$ (2.450 Å), C(9)–H(9C)···S(1)$^{\#1}$ (2.920 Å) and C(9)–H(9A)···Ni (2.620 Å) interactions between adjacent molecules (Fig. 7). Polymeric network of this complex shows the presence of cavities. In complex **2**, interactions between phenyl ring at C(17) carbon atom of one independent molecule with phenyl ring at C(27) carbon atom of the adjacent molecule {C(15)–H(15)···π(C(22)), 2.865; C(15)–H(15)···π(C(21)), 2.763 Å} led to the formation of 1D chain. Two adjacent 1D chains are connected via phenyl groups at N(14) and C(27) atoms {(C(26))···π(C(110)), 3.300; C(10)–H(10)···π(C(26)), 2.826 Å} which formed a 2D sheet (Fig. 8).

Packing diagram of complex **4** shows that 1D chain is formed by interactions between thioamide moiety of one independent dinuclear unit with the phenyl group of PPh$_2$–CH$_2$–PPh$_2$ ligand of the adjacent dinuclear unit {C(19)–H(19)···S(2), 2.881; N(3)–H(3D)···π(C(19)), 2.734 Å}. This 1D chain is linked with the similar chain through C(10)–H(10B)···π(C(22)), 2.865 Å interaction and formed 2D sheet (Fig. 9). Complex **7** exists as a linear H-bonded polymer which is formed through intermolecular interactions between phenyl ring of PPh$_2$–CH$_2$–PPh$_2$ co-ligand and hydrazinic nitrogen atom, C(15)–H(15A)···N(2), 2.450 Å (Fig. 10).

In complex **8**, one molecule is connected with the adjacent molecule via C(10B)–H(8BA)···S, 2.971 and C(1B)–H(1BA)···π(C(1A)), 2.769; C(1B)–H(1BA)···π(C(2A)), 2.784; C(1B)–H(1BA)···π(C(3A)), 2.851; C(1B)–H(1BA)···π(C(4A)), 2.883; C(1B)–H(1BA)···π(C(5A)), 2.873; C(1B)–H(1BA)···π(C(6A)), 2.847 Å interactions, and formed

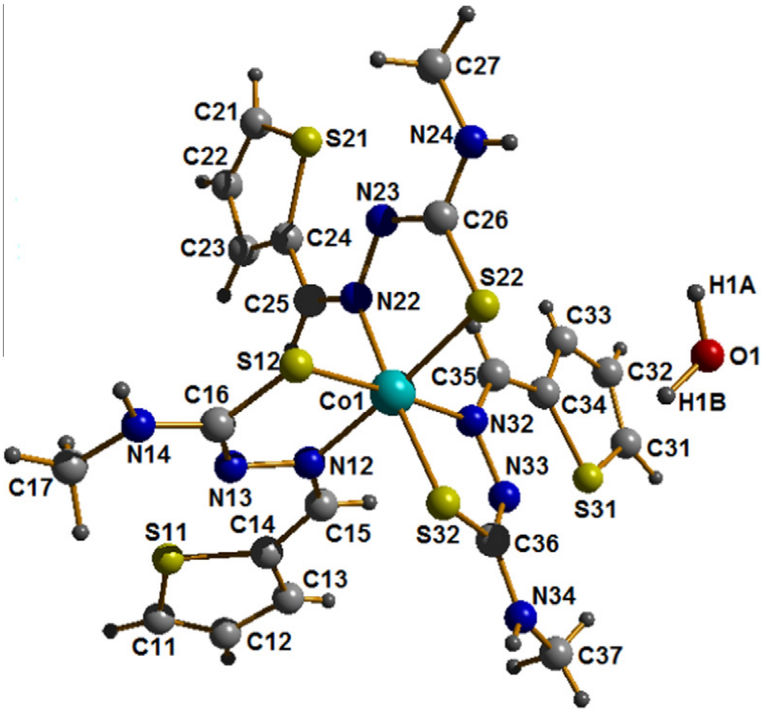

Fig. 6. Molecular structure of complex [Co(κ^2-N, S–HL^8)$_3$] (**9**).

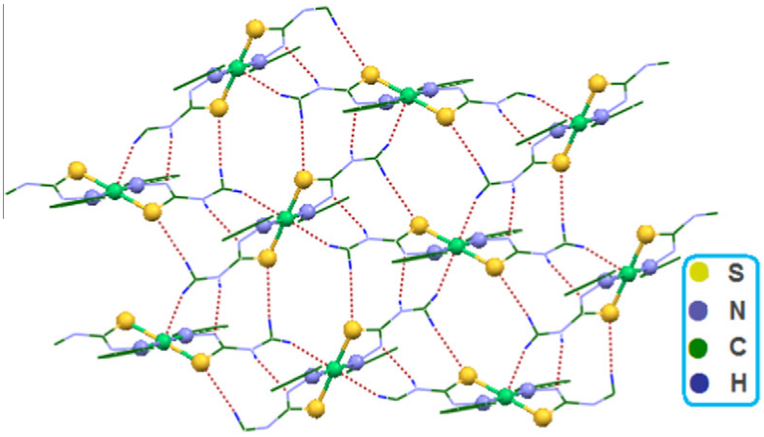

Fig. 7. Packing interactions in complex **1**.

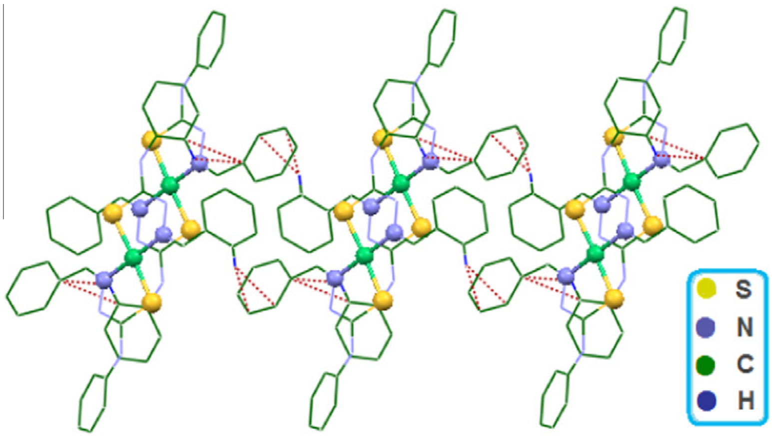

Fig. 8. Packing interactions in complex **2**.

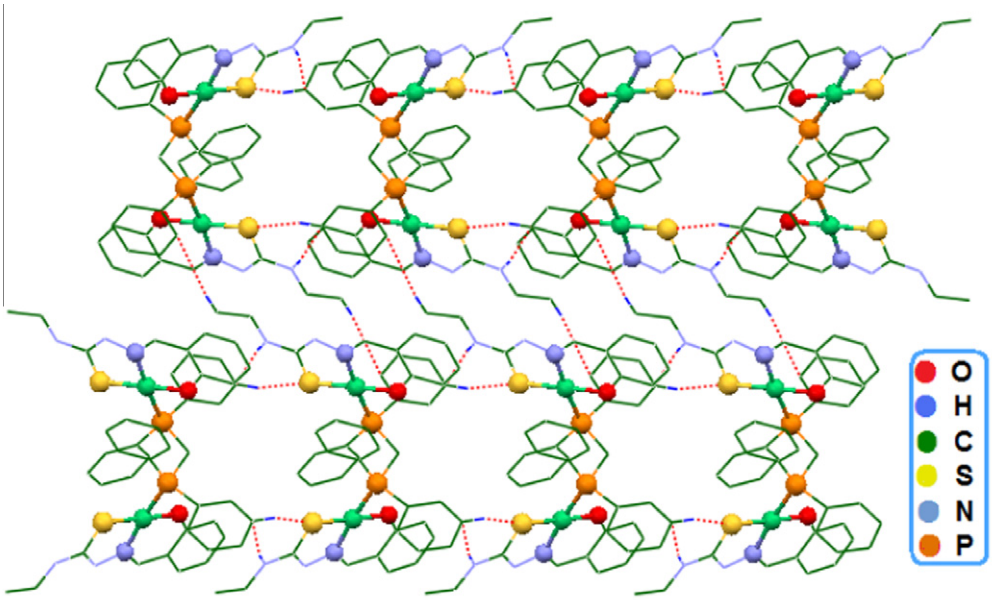

Fig. 9. Packing interactions in complex **4.**

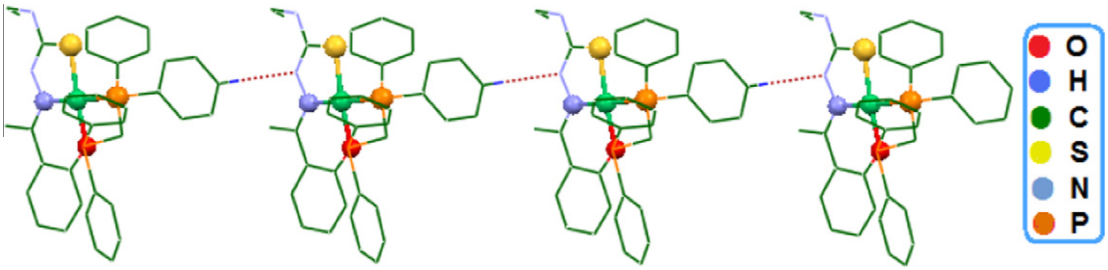

Fig. 10. The intermolecular interactions between adjacent molecules of complex **7.**

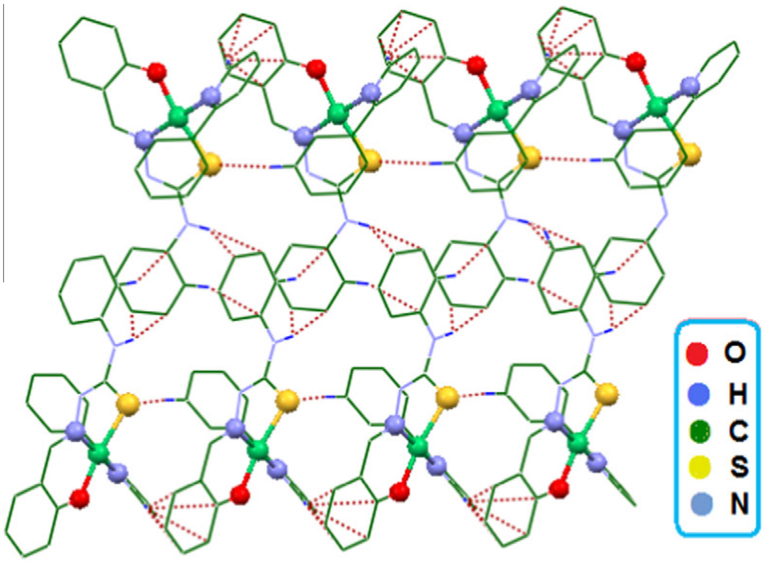

Fig. 11. Packing interactions in complex **8.**

1D polymeric chain. Interactions between these 1D chains through phenyl ring and amino hydrogen {N(3A)–H(3AB)···π(C(12A)), 2.864; N(3A)–H(3AB)···π(C(13A)), 2.725; C(14A)–H(14A)···π(C(9A)), 2.766 Å} formed 2D sheet (Fig. 11).

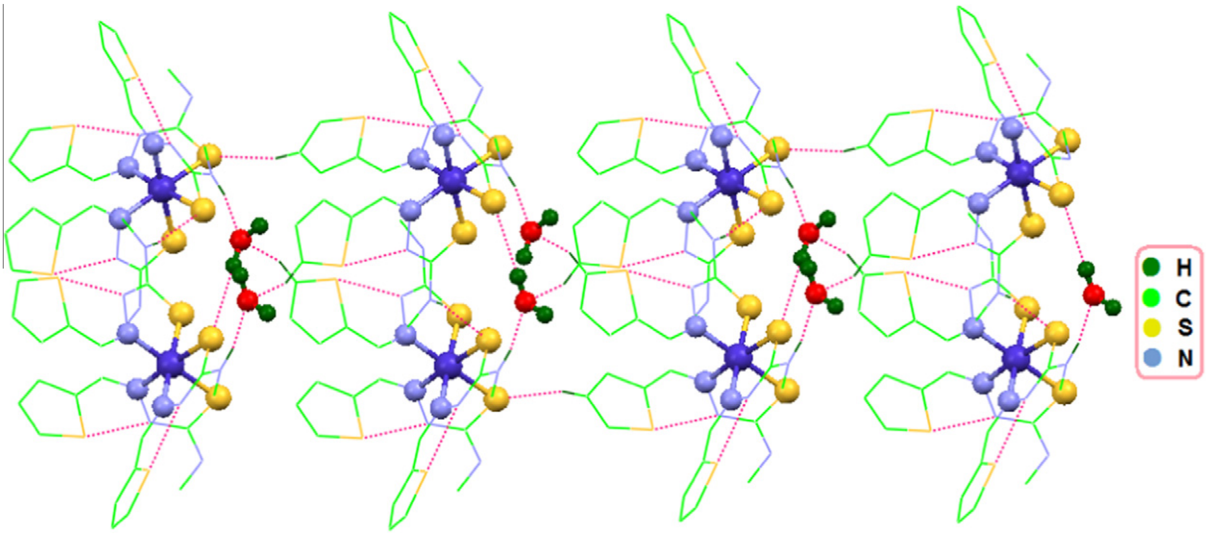

Fig. 12. Packing interactions in complex **9**.

In complex **9**, thiophene ring is engaged in intramolecular interaction with deprotonated hydrazinic hydrogen, S(11)···N(13), 2.745; S(21)···N(23), 2.743; S(31)···N(33), 2.740 Å. One independent molecule interacts with the adjacent molecule either directly {N(14)–H(14A)···S(32), 2.830 Å} or through water molecule present in the crystal lattice {N(34)–H(34A)···O(1), 2.060; O(1)–H(1B)···S(32), 2.850 Å} and formed a dinuclear unit. Two such dinuclear units are connected through water molecule in the lattice via N(34)–H(34A)···O(1), 2.060 and C(11)–H(11)···O(1), 2.613 Å interactions and formed polymeric chain (Fig. 12).

3.4. Solution phase behavior

The ^{1}H NMR spectrum of the free thio-ligand shows a strong signal at δ 9.41 ppm, due to hydrazinic N^{2}H hydrogen. The absence of this signal in complex **1** confirms the deprotonation of N^{2}H hydrogen during complex formation [17]. Further, in this complex, signal due to N^{1}H proton at δ 5.03 ppm showed upfield shift vis-à-vis the free ligand (δ 7.49 ppm). The C^{2}H signal merges with phenyl ring proton C^{4}H and appears as doublet at δ 8.05 ppm. The N^{1}CH$_3$ protons appear as doublet at δ 3.00 ppm and show upfield shift relative to the free ligand (δ 3.27 ppm). Complex **2** showed a similar behavior (see Section 2).

In free ligand, H$_2$L^3, signals due to OH and N^{2}H groups appear at δ 10.95 and 9.61 ppm respectively, but in complex **3**, the disappearance of these proton signals suggested their deprotonation during complexation [20]. The N^{1}H proton signal at δ 4.91 ppm in complex showed upfield shift relative to the free ligand (δ 7.56 ppm). The signals of dppm ligand due to phenyl ring protons are present as multiplets at δ 7.15 ppm and –CH$_2$– protons as singlet at δ 2.86 ppm. The methyl group at N^1 nitrogen {δ 2.10 ppm} moved upfield relative to the free ligand {δ 3.12 ppm}. Complexes **4**–**8** also showed the similar behavior. The characteristic signals due to groups at N^1 and C^2 atoms of these complexes are listed in Section 2.

The most characteristic signal due to N^{2}H group in the free ligands {δ 9.15, H$_2$L^8; 10.80, H$_2$L^9 ppm} is absent in complexes **9** and **10**, which revealed the deprotonation of this group during complexation [17]. The broad signal due to N^{1}H proton in complexes (**9**, δ 5.22; **10**, 5.25, ppm) showed upfield shift relative to the free ligands (δ 7.06, 6.48 ppm). Similarly, C^{2}H signal at δ 7.56 (**9**), 8.53 (**10**) ppm, showed up- and down- field shifts vis-à-vis the free ligands, δ 7.93, 7.86 ppm. The ligand ring protons appear in the range, δ 7.63–6.59 ppm. The N^{1}HCH$_3$ methyl protons appear as a doublet at δ 3.25 (**9**), 3.09 (**10**) ppm.

The ^{31}P NMR spectra of complexes **3**–**7** confirmed the different types of coordination behavior shown by PPh$_2$-CH$_2$-PPh$_2$ co-ligand. In complexes **3**–**5**, a single peak is observed at δ −127.74(**3**), −127.55(**4**), −126.61(**5**) ppm (coordination shift ≈ 35) which demonstrated the equivalence of P atoms of the bridging PPh$_2$–CH$_2$–PPh$_2$ ligand [43]. However, complexes **6** and **7** showed two signals which supported the presence of non equivalent phosphorus atoms in these complexes. The presence of two different peaks is assigned as follows: the signal at δ −166.59 (**6**), −165.14 (**7**) ppm is due to pendant P atom and that at δ −127.73 (**6**), −122.46 (**7**) ppm is due to coordinated P atom of κ^1-PPh$_2$–CH$_2$–PPh$_2$ in these complexes. The coordination shifts ($\Delta\delta$) are 34.94 ppm in **6** and 40.21 ppm in **7** [43].

4. Conclusion

Benzaldehyde thiosemicarbazones (H$_2$L^1, H$_2$L^2) have shown N^3, S-chelation and formed only trans square planar nickel(II) complexes **1** and **2**, a behavior which is similar to that reported with 4-fluorobenzaldehyde thiosemicarbazone [19]. Salicylaldehyde thiosemicarbazones (H$_2$L^3–H$_2$L^7) have formed dppm bridged dinuclear (**3**–**5**) complexes when R^2 substituent at C^2 was hydrogen and mononuclear (**6**, **7**) complexes with one PPh$_2$ group of dppm pendant when R^2 substituent at C^2 was methyl. The difference could be attributed to the enhanced Lewis basicity of thio-ligands coupled with steric effect of methyl group altering the mode of dppm ligand. 2-Pyridylphenyl in **8** behaves in the same way as does pyridine. Complexes **3**–**7** report first examples of nickel(II) complexes of thiosemicarbazones with a diphosphine as a co-ligand. The thio-ligands H$_2$L^8 and H$_2$L^9 have formed tris octahedral complexes **9** and **10** [1].

Acknowledgements

Financial assistance from CSIR, (Letter No. 09/254(0188)/2009-EMR-I), New Delhi is gratefully acknowledged.

Appendix A. Supplementary material

CCDC 863154–863159; contains the supplementary crystallographic data for complexes **1**, **2**, **4** and **7**–**9**. These data can be obtained free of charge from The Cambridge Crystallographic Data Centre via www.ccdc.cam.ac.uk/data_request/cif. Supplementary data associated with this article can be found, in the online version, at http://dx.doi.org/10.1016/j.ica.2012.09.021.

References

[1] T.S. Lobana, R. Sharma, G. Bawa, S. Khanna, Coord. Chem. Rev. 253 (2009) 977.
[2] M. Akbar Ali, S.E. Livingstone, Coord. Chem. Rev. 13 (1974) 115.
[3] M.J.M. Campbell, Coord. Chem. Rev. 15 (1975) 279.
[4] S. Padhye, G.B. Kauffman, Coord. Chem. Rev. 63 (1985) 127.
[5] D.X. West, S. Padhye, P.B. Sonawane, Struct. Bonding (Berlin, Ger.) 76 (1991) 4.
[6] D.X. West, A.E. Liberta, S. Padhye, R.C. Chilkate, P.B. Sonawane, A.S. Kumbhar, R.G. Yerande, Coord. Chem. Rev. 123 (1993) 49.
[7] J.S. Casas, M.S. Garcia-Tasende, J. Sordo, Coord. Chem. Rev. 209 (2000) 197.
[8] J.S. Casas, M.S. Garcia-Tasende, J. Sordo, Coord. Chem. Rev. 193 (1999) 283.
[9] A. Hartwig, T. Schwerdtle, Toxicol. Lett. 127 (2002) 47.
[10] K.S. Kasprzak, F.W. Sunderman Jr., K. Salnikow, Mutat. Res. 533 (2003) 67.
[11] M.B. Ferrari, F. Bisceglie, G. Pelosi, M. Sassi, P. Tarasconi, M. Cornia, S. Capacchi, R. Albertini, S. Pinelli, J. Inorg. Biochem. 90 (2002) 113.
[12] F. Liang, P. Wang, X. Zhou, T. Li, Z.Y. Li, H.K. Lin, D.Z. Gao, C.Y. Zheng, C.T. Wu, Bioorg. Med. Chem. Lett. 14 (2004) 1901.
[13] S.S. Matkar, L.A. Wrischnik, P.R. Jones, U. Hellmann-Blumberg, Biochem. Biophys. Res. Commun. 343 (2006) 754.
[14] J. Garcia-Tojal, J.L. Pizarro, A. Garcia-Orad, A.R. Perez-Sanz, M. Ugalde, A.A. Diaz, J.L. Serra, M.I. Arriortua, T. Rojo, J. Inorg. Biochem. 86 (2001) 627.
[15] L. Ze-Hua, D. Chun-ying, L. Ji-hui, L. Yong-jiang, M. Yu-Hua, Y. Xiao-Zeng, New J. Chem. 24 (2000) 1057.
[16] (a) T.S. Lobana, G. Bawa, G. Hundal, M. Zeller, Z. Anorg. Allg. Chem. 634 (2008) 931;
(b) T.S. Lobana, G. Bawa, A. Castineiras, R.J. Butcher, M. Zeller, Organometallics 27 (2008) 175;
(c) T.S. Lobana, Rekha, R.J. Butcher, A. Castineiras, E. Bermejo, P.V. Bharatam, Inorg. Chem. 45 (2006) 1535;
(d) T.S. Lobana, S. Khanna, G. Hundal, P. Kaur, B. Thakur, S. Attri, R.J. Butcher, Polyhedron 28 (2009) 1583;
(e) T.S. Lobana, S. Khanna, R.J. Butcher, A. Hunter, M. Zeller, Inorg. Chem. 46 (2007) 5826;
(f) T.S. Lobana, P. Kumari, R.J. Butcher, Inorg. Chem. Commun. 11 (2008) 11.
[17] T.S. Lobana, P. Kumari, M. Zeller, R.J. Butcher, Inorg. Chem. Commun. 11 (2008) 972.
[18] T.S. Lobana, P. Kumari, R. Sharma, A. Castineiras, R.J. Butcher, T. Akitsu, Y. Aritake, Dalton Trans. 40 (2011) 3219.
[19] M.B. Ferrari, S. Capacchi, G. Reffo, G. Pelosi, P. Tarasconi, R. Albertini, S. Pinelli, P. Lunghi, J. Inorg. Biochem. 81 (2000) 89.
[20] T.S. Lobana, P. Kumari, G. Hundal, R.J. Butcher, Polyhedron 29 (2010) 1130.
[21] L.E. Nikolaeva, T.N. Tarkhova, N.V. Belov, Kristallografiya (Russ.) (Crystallogr. Rep.) 19 (1974) 746.
[22] E. Gyepes, T. Glowiak, Proc. Conf. Coord. Chem. 11 (1987) 87.
[23] M. Soriano-Garcia, R.A. Toscano, J. Valdes-Martinez, J.M. Fernanadez, Acta Crystallogr., Sect. C 41 (1985) 498.
[24] A. Berkessel, G. Hermann, O.-T. Rauch, M. Buchner, A. Jacobi, G. Huttner, Chem. Ber. 129 (1996) 1421.
[25] J. Valdes-Martinez, S. Hernandez-Ortega, V.B. Jimenez, Acta Crystallogr., Sect. E 58 (2002) m710.
[26] J. Valdes-Martinez, S. Hernandez-Ortega, V.B. Jimenez, Acta Crystallogr., Sect. E 60 (2004) 42.
[27] (a) R. Prabhakaran, R. Karvembu, T. Hashimoto, K. Shimizu, K. Natarajan, Inorg. Chim. Acta 358 (2005) 2093;
(b) Z.-Y. Cao, Z.-P. Deng, S. Gao, Acta Crystallogr., Sect. E 63 (2007) m1961.
[28] Z. Lu, C. White, A.L. Rheingold, R.H. Crabtree, Inorg. Chem. 32 (1993) 3991.
[29] (a) M. Bonamico, G. Dessy, V. Fares, L. Scaramuzza, Cryst. Struct. Commun. 4 (1975) 629;
(b) R.P. John, A. Sreekanth, M.R.P. Kurup, S.M. Mobin, Polyhedron 21 (2002) 2515;
(c) J. Zhao, Y. Zhang, Acta Crystallogr., Sect. E 64 (2008) m1355;
(d) M. Hakimi, R. Takjoo, V. Erfaniyan, E. Schuh, F. Mohr, Trans. Met. Chem. 35 (2010) 959.
[30] T.S. Lobana, A. Sanchez, J.S. Casas, A. Castineiras, J. Sordo, M.S. Garcia-Tasende, E.M.V. Lopaz, J. Chem. Soc., Dalton Trans. (1997) 4289.
[31] G.M. Sheldrick, Acta Crystallogr., Sect. A 64 (2008) 112.
[32] G.M. Sheldrick, SHELXTL-PC, release 5.03, Siemens Analytical X-ray Instruments Inc., Madison, WI, USA, 1995.
[33] G.X. Win, L.J. Farrugia, J. Appl. Crystallogr. 32 (1999) 837.
[34] G.M. Sheldrick, SADABS, Program for Empirical Absorption Correction of Area Detector Data, University of Goettingen, Germany, 1997.
[35] Oxford Diffraction, CrysAlisPro CCD and CrysAlisPro RED Oxford Diffraction Ltd., Yarnton, England, 2009.
[36] Bruker, SMART and SAINT, Area Detector Control and Integration Software, Bruker Analytical X-ray Instruments Inc., Madison, WI, USA, 1997.
[37] A.J.C. Wilson, International Tables for Crystallography, vol. C, Kluwer Academic Publishers, Dordrecht, The Netherlands, 1995.
[38] A.L. Spek, J. Appl. Crystallogr. 36 (2003) 7.
[39] E. Keller, SCHAKAL-97, A Computer Program for the Graphic Representation of Molecular and Crystallographyc Models, University of Freiburg, Germany, 1997.
[40] (a) P.S. Zhao, H.Y. Wag, J. Song, L.D. Lu, Struct. Chem. 21 (2011) 977;
(b) H.Y. Wang, P.S. Zhao, J. Song, R.Q. Li, J. Chem. Cryst. 41 (2011) 379;
(c) R. Gil-Gercia, R. Zichner, V. Diez-Gomez, B. Donnadieu, G. Madariaga, M. Insausti, L. Lezama, P. Vitoria, M.R. Pedrosa, J. Garcia-Tojal, Eur. J. Inorg. Chem. (2010) 4513.
[41] J.E. Huheey, E.A. Keiter, R.L. Keiter, Inorganic Chemistry Principles of Structure and reactivity, fourth ed., Harper Collins, New York, 1993.
[42] P.F. Rapheal, E. Manoj, M.R.P. Kurup, E. Suresh, Polyhedron 26 (2007) 607.
[43] T.S. Lobana, G. Bawa, G. Hundal, R.J. Butcher, A. Castineiras, Z. Anorg. Allg. Chem. 635 (2009) 1447.